Exchange interaction and spin correlations in donor-magnetic-impurity systems in $Cd_{1-x}Mn_xS$ crystals

D. L. Alov, S. I. Gubarev, and V. B. Timofeev

Institute of Solid State Physics, Academy of Sciences of the USSR
(Submitted 20 September 1982)
Zh. Eksp. Teor. Fiz. **84**, 1806–1816 (May 1983)

The method of spin-flip Raman scattering is used to study the spin correlations in a donor-electron + magnetic-impurity system in the semimagnetic semiconductor $Cd_{1-x}Mn_xS$ ($x = 0.005$). It is shown that the exchange interaction with the magnetic impurity not only increases the paramagnetic susceptibility of the donor electron but also splits its spin state in the absence of a magnetic field. This splitting amounts to $\simeq 7\text{cm}^{-1}$ at $T = 1.8$ K and decreases with increasing temperature. The splitting of the spin state of the donor is accompanied by an ordering of the magnetic moments of the Mn atoms within the volume of the donor wave function. The magnetic moment of the magnetic-impurity subsystem that is associated with the donor is determined from the degree of circular polarization of the Stokes component of the spin-flip Raman scattering and is found to be $\simeq 40\mu_B$ for $x = 0.005$ and $T = 1.8$ K.

PACS numbers: 75.30Et, 75.30.Hx, 75.25. + x, 78.30.Gt

§1. INTRODUCTION

Mixed solid solutions of magnetic and nonmagnetic semiconductors are usually called semimagnetic semiconductors.[1] What is generally meant are $A^{II}B^{VI}$ semiconductor compounds in which a fraction of the cations are replaced by Mn atoms. Examples of semimagnetic semiconductors are $Cd_{1-x}Mn_xTe$, $Cd_{1-x}Mn_xSe$, and $Cd_{1-x}Mn_xS$.[2–5] The presence of localized magnetic moments due to the uncompensated d electrons of Mn in the matrix of these semiconductors leads to anomalous magnetic properties even at low concentrations of the magnetic impurity ($x \sim 10^{-2} - 10^{-3}$), where the band structure and band parameters of the compounds are not yet markedly different from those of the base semiconductor. The strong s–d and p–d exchange interaction between the spins of the nonequilibrium carriers (electrons and hole) and the magnetic moments localized at the magnetic-impurity atoms leads to a giant increase in the paramagnetic susceptibility of the carriers in semimagnetic semiconductors at liquid-helium temperatures. The spin splittings at mole fractions of the order of 10^{-2} Mn can reach[3] tens of meV, values corresponding to an effective g factor of $g = 20$–30. The change of the energy spectrum of the semimetallic semiconductors $Cd_{1-x}Mn_xS$ and $Cd_{1-x}Mn_xSe$ (with the wurtzite structure) as a result of the exchange interaction with the magnetic-impurity subsystem was investigated in Refs. 4 and 5. These papers give an explanation in terms of the effective-molecular-field approximation for a number of anomalous magnetooptic effects observed in hexagonal semimagnetic semiconductors and provide estimates of the values of the exchange integrals.

A convenient tool for investigating exchange effects in semimagnetic semiconductors is inelastic Raman light scattering, by the weakly bound electrons, of a shallow donor impurity, accompanied by a flip of the spin of the donor electron (spin-flip Raman scattering, SFRS). Since this scattering process changes the spin state of the electron, the spectral shift of the SFRS lines is directly related to the spin splitting of the donor state. The first SFRS experiments in $Cd_{1-x}Mn_xS$ (Ref. 6) and $Cd_{1-x}Mn_xSe$ (Ref 7). have shown that the exchange interaction with the magnetic-impurity subsystem causes an initial spin splitting of the donor state, which is manifested in the SFRS spectra as a finite spectral shift of the SFRS line in zero magnetic field. The temperature dependence of this shift gives an explicit indication of the importance of spin correlations in the shallow-donor + magnetic-impurity system and of the possible ordering of the Mn magnetic moments interacting with the donor electron. In this paper we investigate these correlations with the aid of determining the magnetic-impurity-subsystem effective magnetic moment that is associated with an individual donor. The effective magnetic moment can be measured experimentally by studying the SFRS in the Faraday geometry (with the observation direction along the magnetic field). In this case the Stokes and anti-Stokes components of the SFRS are circularly polarized. The depolarization of the SFRS in weak magnetic fields is due to the deviation of the exchange field associated with the effective magnetic moment of the magnetic-impurity subsystem from the direction of the external magnetic field; the degree of circular polarization serves as a measure of this deviation. By studying the dependence of the degree of circular polarization of the SFRS on the magnitude of the external magnetic field, one can measure the magnetic susceptibility of the donor + magnetic-impurity system in CdMsS and thus determine the effective magnetic moment associated with the donor.

§2. EXPERIMENTAL TECHNIQUES

The $Cd_{1-x}Mn_xS$ crystals used in this study were grown from the melt by the Bridgman method. The Mn mole fraction, determined by atomic-absorption analysis, was $x \simeq 5 \cdot 10^{-3}$, corresponding to a concentration $N_{Mn} \simeq 10^{20}$ cm^{-3}[4]. At room temperature the samples had n-type conductivity. The carrier concentration, according to Hall measurements, was $N_D - N_A \simeq 2 \cdot 10^{16}$ cm^{-3}. Samples with di-

 0038-5646/83/051052-07$04.00

mensions of $3\times3\times5$ mm were cut from the $Cd_{1-x}Mn_xS$ single crystal in such a way that the hexagonal axis C_6 of the crystal was normal to the large face of the sample. The samples were mechanically polished and then placed in an optical cryostat inside a superconducting solenoid. Magnetic fields up to 40 kOe were used in this study.

The excitation of the crystal was provided by a cw Ar^+ laser. Predominant use was made of two lines of the Ar^+ laser: $\lambda = 4965$ Å and $\lambda = 5017$ Å, which fall in the transparency region of the crystal near the exciton-absorption edge and give rise to a nearly resonant SFRS process. The maximum power of the emission in these lines was $P \simeq 200$ mW.

In the Voight geometry the sample was placed in the solenoid in such a way that $\mathbf{C}_6 \perp \mathbf{H}$; here the excitation was applied either normal to the surface of the crystal (backscattering) or through a lateral face (90° scattering).

The layout of the apparatus for studying the SFRS spectra in the Faraday geometry is shown in Fig. 1. Since CdS is a uniaxial crystal, the detection of the circularly polarized SFRS light must be done along the crystal axis $\mathbf{k}_s \| \mathbf{C}_6 \| \mathbf{H}$. The excitation in this case was in the π polarization through a lateral face of the sample. The light scattered into the magnetic-field direction along the axis of the crystal was directed to the exit window of the cryostat with the aid of a glass 45-degree total-internal-reflection prism placed above the sample. The excited region, which formed a vertical strip 5-mm wide and 100-μm long in the image plane, was then focused by a lens onto the entrance slit of the spectroscopic device. A $\lambda/8$ plate compensated the phase difference introduced by the total-internal-reflection prism. An analyzer for circularly polarized light, which was a polarizer combined with a quarter-wave plate, permitted recording of the SFRS spectra in the σ^+ and σ^- polarizations.

The spectroscopic device was a DFS-24 double monochromator having diffraction gratings with 1200 lines/mm and a linear dispersion of 4.5 Å/mm, giving a resolution of 1 cm^{-1} or better for 30-μm slits. Photoelectric detection was provided by a liquied-nitrogen-cooled FEU-79 photomultiplier operating as a photon counter.

The measurements above 4.2 K were made with the aid of a special insert—a hermetic cell with small windows, in which the sample and a deflecting prism were placed. The temperature of the sample was changed by a heater. The temperature was monitored with a calibrated germanium thermistor.

The useful SFRS signal for 30×30-μm spectral slits was at the level of $3\cdot10^4$ counts/sec in the case of the Voigt configuration and $5\cdot10^3$ counts/sec in the Faraday configuration.

§3. EXPERIMENTAL RESULTS

In CdS crystals without a magnetic impurity the SFRS spectrum appears as very narrow Stokes and anti-Stokes components which are spectrally split off from the Rayleigh line by an amount $\mu_B g_D H$, with a donor-electron g factor $g_D = 1.76$ (Ref. 8). In Mn-doped crystals the spectral shift of the SFRS lines is significantly larger (Fig. 2). The dependence of the exchange field on the parameter H/T leads to saturation of the spectral shift $\Delta\nu(H)$ in the region of large magnetic fields. Thus illustrating the magnetic-field dependence of the magnetization of the magnetic-impurity subsystem. The SFRS line in $Cd_{1-x}Mn_xS$ is appreciably broadened in comparison with that of pure CdS. Its half-width in small magnetic fields amounts to 1.5 Å and increases to 2.2 Å in saturating magnetic fields. The appreciable width of the SFRS line is evidently due to inhomogeneity of the Mn distribution in the sample and to thermal fluctuations of the magnetization of the magnetic-impurity subsystem within the volume of the wave function of each individual donor.

The most interesting behavior of the SFRS line occurs in small magnetic fields. As the field becomes weaker, the spectral shift $\Delta\nu$ decreases; however, it does not go to zero at $H = 0$, but remains finite. This is evidence of an initial spin splitting of the donor state even in the absence of magnetic field.

As the temperature of the crystal rises, the spectral shift of the SFRS line decreases, as does the size of the residual splitting in zero magnetic field. At high temperatures, beginning at approximately 6 K, the anti-Stokes component of the

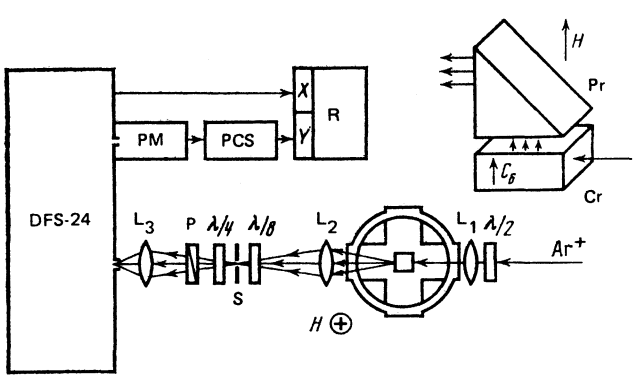

FIG. 1. Schematic of experimental apparatus for observing SFRS in the Faraday configuration: L_1, L_2, and L_3 are lenses; $\lambda/2$, $\lambda/4$, $\lambda/8$ are phase plates; P is a polarizer; S is an intermediate slit; PCS is a photon-counting system; R is an xy recorder. In the upper right-hand corner is a diagram of the experimental geometry; Pr is a 45-degree glass prism and Cr is the sample.

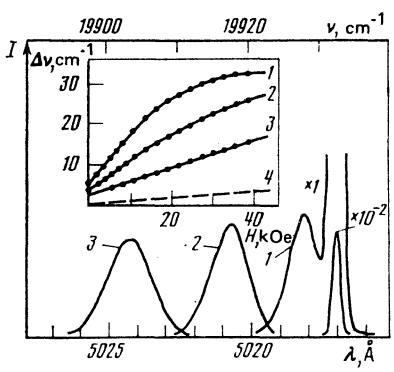

FIG. 2. SFRS spectra in $Cd_{1-x}Mn_xS$ ($x = 0.005$) in magnetic fields: 1) $H = 0$, 2) $H = 8.5$ kOe, 3) $H = 30$ kOe. Excitation is by the $\lambda = 5017$-Å line at a power $P = 100$ mW. The temperature is $T = 2$ K. The inset shows the magnetic-field dependence of the spectral shift $\Delta\nu(H)$ of the SFRS line at temperatures: 1) $T = 2$ K, 2) $T = 4.2$ K, 3) $T = 13$ K. The dashed line (4) shows the dependence of the spectral shift $\Delta\nu(H)$ in pure CdS.

SFRS begins to appear on the high-energy side of the Rayleigh line. The intensity ratio of the Stokes and anti-Stokes components is well described in terms of the temperature of the crystal, and this is evidence that the different spin states of the donor are in thermodynamic equilibrium.

The anti-Stokes component of the SFRS is characterized by a smaller spectral shift than that of the Stokes component. As the temperature rises, the difference between the spectral positions of the Stokes and anti-Stokes peaks becomes smaller, and at temperatures of the order of 20 K the spectral shifts of the SFRS components practically coincide.

The fact that the spin splitting of the donor state in zero magnetic field is temperature dependent indicates an ordering of the Mn magnetic moments within the volume of the donor and the formation of an effective magnetic moment associated with the donor electron in the magnetic-impurity subsystem. In order to study this effective moment we made polarization measurements of the SFRS in the Faraday geometry (Figs. 3, 4). In this case the SFRS line is circularly polarized, with opposite signs of the circular polarization for the Stokes and anti-Stokes components. At low temperatures $T \leqslant 2$K the circular polarization of the SFRS line is complete even in fields as low as $\simeq 3$ k0e. As the magnetic field is reduced, the component of the opposite polarization begins to appear in the SFRS spectrum (Fig. 4,b,c), and at $H = 0$ the line is completely depolarized. Reversing the magnetic field reverses the sign of the circular polarization of the SFRS. The degree of circular polarization p of the Stokes components of the SFRS is not constant over the bandwidth—it decreases toward the edge of the spectrum nearer the laser and increases toward the far edge. This causes the spectral positions of the Stokes peak in the SFRS to be different in the σ^+ and σ^- polarizations. As the polarization of the SFRS decreases, there is a leveling of the difference in the spectral positions.

At higher temperatures the behavior of the polarization properties of the SFRS remains qualitatively the same, except that the onset of the circular polarization occurs at higher values of the magnetic field.

The degree of polarization of the SFRS is related to the orientation of the effective magnetic moment associated with the donor, while the size of the initial splitting of the donor state is related to the magnitude of this moment. With rising temperature the effective moment of the magnetic-impurity subsystem decreases in magnitude, and the zero-field spectral shift $\Delta\nu(H = 0)$ along with it, and at high temperatures the SFRS line is not resolved (Fig. 5).

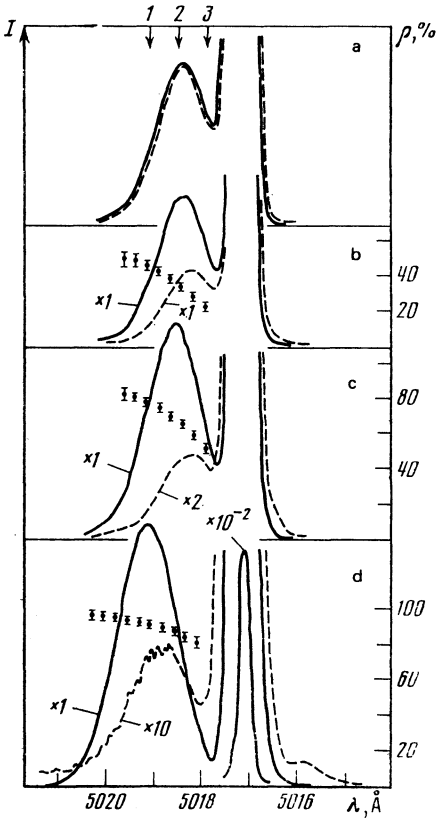

FIG. 4. SFRS spectra in $Cd_{1-x}Mn_xS$ recorded in the polarizations σ^+ (solid curve) and σ^- (dashed curve) in magnetic fields: a) $H = 0$ kOe, b) $H = 0.5$ kOe, c) $H = 1.3$ kOe, d) $H = 2.5$ kOe. The temperature of the sample was $T = 1.8$ K. The points give the degree of circular polarization ρ of the Stokes component of the SFRS.

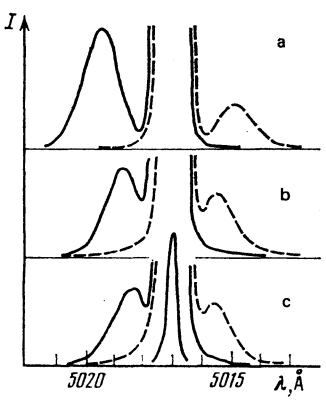

FIG. 3. SFRS spectra in $Cd_{1-x}Mn_xS$, recorded in the polarizations σ^+ (solid curves) and σ^- (dashed curves) in a field $H = 17$ kOe at temperatures: a) $T = 12$ K, b) $T = 21$ K, c) $T = 30$ K. Excitation $\lambda = 5017$ Å, $P = 100$ mW.

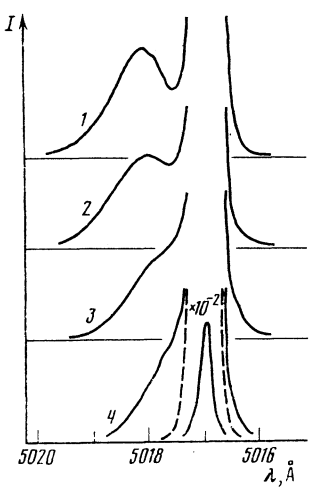

FIG. 5. SFRS spectrum in $Cd_{1-x}Mn_xS$ in zero magnetic field at temperatures: 1) $T = 2$ K, 2) $T = 4.2$ K, 3) $T = 10$ K, 4) $T = 28$ K.

In summary, the main experimental features of the SFRS in $Cd_{1-x}Mn_xS$ can be formulated as follows:

1) The spectral shift of the SFRS line is anomalously large in comparison with pure CdS and is saturable in large magnetic fields; the linewidth is substantially larger than in pure CdS.

2) As the temperature is raised, the size of the spectral shift decreases, and the anti-Stokes component of the SFRS sets in; the spectral shift of the anti-Stokes component is smaller than that of the Stokes component.

3) In zero magnetic field there is an initial splitting of the donor state, which decreases in size as the temperature is raised.

4) In the Faraday geometry the SFRS line is unpolarized at $H = 0$, but becomes substantially polarized even in small magnetic fields; the signs of the circular polarization of the Stokes and anti-Stokes components of the SFRS are opposite.

5) The degree of circular polarization is not constant within the SFRS bandwidth, but increases with distance from the laser line.

§4. DISCUSSION OF EXPERIMENTAL RESULTS

For the spin-flip Raman scattering of light by conduction electrons, Yafet,[9] using states in the valence band as intermediate states, obtained the following expression for the scattering cross section:

$$\left(\frac{d\sigma}{d\Omega}\right)_{ij}=\frac{e^2}{mc^2}\left[\frac{1}{m}\sum_{k}\frac{(\mathbf{e}_s\mathbf{p})_{jk}(\mathbf{e}_L\mathbf{p})_{ki}}{E_i-E_k+\hbar\omega_L}+\frac{(\mathbf{e}_L\mathbf{p})_{jk}(\mathbf{e}_s\mathbf{p})_{ki}}{E_i-E_k-\hbar\omega_s}\right]^2; \quad (1)$$

here $\mathbf{e}_L$ and $\mathbf{e}_s$ are unit vectors describing the polarization of the incident and scattered light, ω_L and ω_s are the frequencies of the incident and scattered light ($\hbar\omega_s = \hbar\omega_L \pm \Delta E^e$), m is the electron mass, and $\mathbf{p}$ is the momentum operator. The summation is over all intermediate states. In the case of CdS these are the states of the A, B, and C valence bands.

In SFRS the electron changes its spin state, so the size of the spectral shift of the SFRS line is a direct reflection of the size of the spin splitting of the electron state. The exchange interaction with the magnetic moments of the Mn atoms appreciably alters the energy of the spin states of the electrons in the conduction band:

$$E^{\pm}=E^0\pm{}^1/_2N_0x\alpha\langle S_{Mn}{}^z\rangle_{H,T}. \quad (2)$$

Here N_0 is the number of cation states in a unit volume of the crystal, x is the mole fraction of Mn, α is the constant describing the exchange interaction of a conduction electron with a manganese atom, and the last factor in (2) is the average value of the magnetization of the magnetic-impurity subsystem. At mole fractions $x \leqslant 1\%$ the average distance between Mn atoms is several lattice constants. In this case the direct Mn–Mn interaction can be neglected, and the magnetization is relatively well described by a Brillouin function $B_j(t)$ with $j = 5/2$, i.e.,

$$\langle S_{Mn}{}^z\rangle_{H,T}=B_{5/2}(\mu_B g_{Mn}H/T). \quad (3)$$

It is this exchange interaction which is responsible for the anomalously large spectral shift of the SFRS line that is observed in $Cd_{1-x}Mn_xS$ in a magnetic field at liquid-helium temperatures. The saturation of the spectral shift $\Delta\nu(H)$ of the SFRS line in large magnetic fields and the decrease of $\Delta\nu$ with increasing temperature are governed by the H and T dependence of the average magnetization of the magnetic-impurity subsystem.

The presence of spin splitting of the donor state in zero magnetic field and the temperature dependence of this splitting indicate that the donor is surrounded by a spontaneous exchange field due to the local polarization of the magnetic-impurity subsystem. The role of the exchange interation in shaping the energy spectrum of the shallow-neutral-donor + magnetic-impurity system has been studied theoretically by several authors for the case of ferromagnetic and antiferromagnetic semiconductors.[10,11] The variational methods developed by Krivoglaz,[10] which take into account the fluctuations of the magnetization of the magnetic-impurity subsystem, were recently applied to the case of a semimagnetic semiconductor by Dietl and Spalek.[12] The basic idea of these calculations is to take into account not only the exchange field of the magnetic-impurity subsystem which polarizes the donor electron, but also the inverse effect, i.e., the exchange filed G_M of the donor electron which polarizes the magnetic-impurity subsystem. This field is proportional to the probability of finding an electron in a crystal containing manganese atom, namely

$$G_M\infty|\psi_e(\mathbf{r})|^2\sim\exp(-2r/a_B),$$

where a_B is the Bohr radius of the neutral donor.

The spin splitting of the donor state and the average value of the magnetization $\mathbf{M}(\mathbf{r})$ of the magnetic-impurity subsystem are obtained through a self-consistent calcualtion of both these fields.

Let

$$\mathbf{M}(\mathbf{r})=g_{Mn}\mu_B\mathbf{S}_i\delta(\mathbf{r}-\mathbf{r}_i)$$

be the distribution of the magnetic moments of the Mn atoms in the lattice of the semiconductor as obtained from such a self-consistent solution. The magnitude of the exchange field acting on an electron will then be[12]

$$G_e=\alpha\int\mathbf{S}(\mathbf{r})|\psi_e(\mathbf{r})|^2\,d\mathbf{r}=\frac{\alpha}{g\mu_B}\int\mathbf{M}(\mathbf{r})|\psi_e(\mathbf{r})|^2\,d\mathbf{r}. \quad (4)$$

This field corresponds to an effective magnetic moment of the magnetic-impurity subsystem

$$\mathbf{M}_{\text{eff}}=\int\mathbf{M}(\mathbf{r})|\psi_e(\mathbf{r})|^2d\mathbf{r}.$$

If the variation, due to thermal fluctuations, of $\mathbf{M}_{\text{eff}}$ about its equilibrium value is slow enough, the donor electron will adiabatically follow this variation. The splitting of the donor state in this case will be proportional to $|M_{\text{eff}}|$, and the spin of the donor electron will be polarized in the direction of $\mathbf{M}_{\text{eff}}$. Under these assumptions the shape and position of the SFRS line reflect the statistical distribution of the effective magnetic moments over their absolute value $|M_{\text{eff}}|$.

The degree of circular polarization at fixed frequencies within the SFRS spectrum will therefore reflect the angular distribution of the effective magnetic moments with a given value of $|M_{\text{eff}}|$.

As the temperature of the crystal is lowered, the role of the spin correlations in the donor- + -magnetic-impurity system becomes increasingly important, and the magnetic-impurity subsystem becomes more highly polarized. This leads to a shift of the distribution of M_{eff} toward larger values of the effective magnetic moment, and this is manifested in the SFRS spectrum as an increase in the spectral shift of the SFRS line in zero magnetic field.

The SFRS linewidth in $Cd_{1-x}Mn_xS$ is governed by the scatter in the absolute values of the effective magnetic moment associated with different donor states. The main causes of this scatter are:

1) The inhomogeneity of the Mn distribution, i.e., the random nature of the positions of the Mn atoms in the lattice of the semiconductor,

2) Thermal fluctuations of the magnetization of the magnetic-impurity subsystem for a given configuration of the Mn distribution in the crystal. For magnetic fields in the saturation region the magnetic-impurity subsystem is completely polarized and the thermal fluctuations of the magnetization are equal to zero. In this case the SFRS linewidth is determined exclusively by the inhomogeneity of the Mn distribution in the crystal. As the magnetic field is decreased in strength the role of the inhomogeneities is substantially reduced, while the thermal fluctuations grow in size. Thus, both mechanisms contribute to the SFRS linewidth in the region of small magnetic fields.

Let us consider how the scatter in $|M_{\text{eff}}|$ influences the line shape and the intensity of the anti-Stokes component of the SFRS. The Stokes $I_S(\nu_0-\Delta\nu)$ and anti-Stokes $I_a(\nu_0+\Delta\nu)$ components of the SFRS, which are shifted with respect to Rayleigh line by an amount $\Delta\nu$, correspond to a transition between spin states of the donor which are split by the exchange interaction by an amount $\Delta E^e = h\Delta\nu$. The intensity of the anti-Stokes component will in this case be weaker than that of the Stokes component in proportion to the Boltzmann factor, which reflects the population of the spin states of the donor electron, i.e.,

$$I_a(\nu_0+\Delta\nu)=I_c(\nu_0-\Delta\nu)\exp(-h\Delta\nu/T). \tag{5}$$

This accounts for the observed difference in the spectral positions of the Stokes and anti-Stokes peaks in the SFRS (Fig. 6).

Let us turn now to the polarization measurements made in the Faraday geometry. In the absence of magnetic field the effective magnetic moments associated with the different donor states are directed at random, and the SFRS line is unpolarized. A magnetic field orients these moments and gives rise to a circular polarization of the scattered light. Large values of the spectral shift $\Delta\nu$ correspond to large values of the effective moment M_{eff}, and so the degree of polarization of the SFRS should increase with distance from the Rayleigh line of the laser, in agreement with the experimental results (Fig. 4).

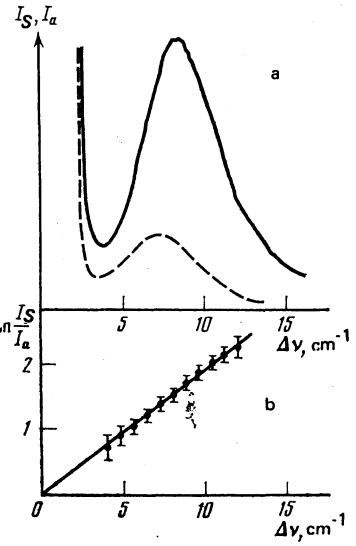

FIG. 6. a) Intensity of Stokes (solid curve) and anti-Stokes (dashed curve) component of SFRS as a function of the size of the spectral shift $\Delta\nu$ from the laser line. $H = 12$ kOe, $T = 8$ K. Excitation $\lambda = 4965$ Å, $P = 200$ mW. b) Intensity ratio of Stokes and anti-Stokes components of the SFRS as a function of the spectral shift $\Delta\nu$.

The angular distribution of the magnetic moments $\mathbf{M}_{\text{eff}}$ in a magnetic field $\mathbf{H}$ is given by the formula

$$P(M_{\text{eff}},\theta)\,d\Omega = Z\exp(M_{\text{eff}}H\cos\theta/T)\,d\Omega,$$
$$Z=\left(\int\exp(M_{\text{eff}}H\cos\theta/T)\,d\Omega\right)^{-1}. \tag{6}$$

If the SFRS matrix element is independent of the angle, i.e., $|M_{\text{SFRS}}|^2 = \text{const}$, then the degree of circular polarization of the scattered light is described by the Langevin function $L(t)$:

$$\rho=\langle\cos\theta\rangle = M^z_{\text{eff}}/M_{\text{eff}} = L(M_{\text{eff}}H/T),$$
$$L(t)=\text{cth}(t)-1/t. \tag{7}$$

Allowance for the angular dependence of $|M_{\text{SFRS}}|^2$, however, substantially alters the form of $\rho(H)$.

In the case of the Faraday geometry, the light was detected along the C_6 axis in the σ^+ polarization, while the excitation was in the π polarization, so that $\mathbf{e}_L \| \mathbf{C}_6$. In this case the states in the A band are spectroscopically inactive, and the intermediate states for the SFRS process are those in the valence subbands B and C.

In principle, the exchange interaction can substantially alter the energy spectrum and wave functions of the electrons of the valence band.[4,5] However, in the low-field region, where the polarization measurements were made, the splittings of the valence band are small compared to the crystalline-field constant Δ_{cr} and spin-orbit interaction constant Δ_{so}. One may therefore neglect the change in the energy denominator in (1) due to the exchange field and use for the wave functions of the intermediate states the unperturbed wave functions of the B and C bands of CdS. These functions are of the form

$$\psi_B^1 = C_1 X^+\downarrow + C_2 z\uparrow, \quad \psi_C^1 = -C_2 X^+\downarrow + C_1 z\uparrow,$$
$$\psi_B^2 = C_1 X^-\uparrow + C_2 z\downarrow, \quad \psi_C^2 = -C_2 X^-\uparrow + C_1 z\downarrow, \tag{8}$$

where $X\pm = 2^{-1/2}(x \pm iy)$; x, y, and z transform like the atomic functions p_x, p_y, and p_z and $C_1^2 = 0.54$ and $C_2^2 = 0.46$ for CdS (Ref. 4).

If $\mathbf{M}_{\text{eff}}$ (and, accordingly, the electron spin σ) forms an angle θ with the C_6 axis of the crystal, one can write the electron states in the following form (omitting the spatial part of the wave function):

$$|S^1\rangle = -\cos(\theta/2)\,|\uparrow\rangle + \sin(\theta/2)\,|\downarrow\rangle,$$
$$|S^2\rangle = -\sin(\theta/2)\,|\uparrow\rangle + \cos(\theta/2)\,|\downarrow\rangle. \tag{9}$$

The matrix elements for spin-flip Raman scattering from state S^1 to state S^2 (the Stokes component) through intermediate state ψ_B^1 are written

$$M_S^+ = \langle S^1|e_L^z|\psi_B^1\rangle\langle\psi_B^1|e_s^+|S^2\rangle = C_1 C_2 M^2 \cos^2(\theta/2),$$
$$M_S^- = \langle S^1|e_L^z|\psi_B^1\rangle\langle\psi_B^1|e_s^-|S^2\rangle = 0. \tag{10}$$

The matrix elements for SFRS via the intermediate states ψ_B^2, ψ_C^1, and ψ_C^2 are calculated in a similar way. The summation over all intermediate states leads to the following dependence for the SFRS intensities:

$$I_c^+ \propto \cos^4(\theta/2), \quad I_c^- \propto \sin^4(\theta/2). \tag{11}$$

Using these expressions together with distribution function (6), we obtain

$$I_S^+ = Z\int \cos^4(\theta/2)\exp(M_{\text{eff}} H\cos\theta/T)\,d\Omega,$$
$$I_S^- = Z\int \sin^4(\theta/2)\exp(M_{\text{eff}} H\cos\theta/T)\,d\Omega. \tag{12}$$

The degree of polarization of the Stokes component of the SFRS at the frequency $\nu = \nu_0 - \Delta\nu$ will be

$$\rho = \frac{I^+ - I^-}{I^+ + I^-} = W(x) = \frac{x(x\,\text{cth}\,x - 1)}{x^2 + 1 - x\,\text{cth}\,x}, \quad x = \frac{M_{\text{eff}} H}{T}. \tag{13}$$

The function W can be expressed in terms of the Langevin function as

$$W(x) = \frac{xL(x)}{x - L(x)}. \tag{14}$$

The function $W(x)$ behaves like $L(x)$ in the saturation region $x >> 1$, but has a different expansion about $x = 0$, i.e., $W(x) \simeq x/2$, whereas $L(x) \simeq x/3$.

Taking several spectral points within the SFRS bandwidth (denoted by arows 1, 2, and 3 in Fig. 4), plotting the degree of circular polarization of the SFRS versus the magnetic field at these points, and approximating these curves by the function $W(x)$, one can determine the magnitude of the effective magnetic moment associated with the donor (Fig. 7). At the peak of the SFRS line, corresponding to the most probable configuration of magnetic moments, approximation by $W(x)$ gives a value $M_{\text{eff}} \simeq 40\mu_B$, corresponding to the combined moment of approximately eight Mn atoms. Thus, the experimental dependence can be described well in terms of an effective magnetic moment associated with the donor electron, and the magnitude of this moment can be determined experimentally on the basis of polarization measurements in a longitudinal magnetic field.

The experiments on SFRS in $Cd_{1-x}Mn_xS$ permits us to refine the value of the exchange integral α describing the interaction of the magnetic moment of the Mn atoms with the conduction electrons, which was previously estimated in magnetooptic studies of the excition reflection spectra.[4] Using the value of the spin splitting $\Delta E_{\text{sat}}^e \simeq 4$ meV in saturating magnetic fields at a magnetic-impurity concentration $N_{\text{Mn}} \simeq 10^{20}\text{cm}^{-3}$, we obtain in accordance with formula (2) the value $N_0\alpha = (0.3 \pm 0.03)$ eV.

We did not measure the absolute sign of the circular polarization of the SFRS in $Cd_{1-x}Mn_xS$. The sign of the exchange interaction of the conduction electrons with the Mn atoms in these crystals thus remains an open question.

§5. CONCLUSION

The model we have used to describe the exchange interaction in the donor + magnetic-impurity system is a qualitative one. We consider it very important to do more detailed calculations of the energy spectrum of such a system with allowance for the inhomogeneity of the Mn distribution in the crystal and for thermal fluctuations of the magnetization in order to obtain the shape and width of the SFRS spectrum in semimetallic semiconductors and determine the spontaneous magnetization of the magnetic-impurity subsystem as a function of temperature and the distance from the center of the donor.

From an experimental standpoint it is extremely interesting to study semimetallic semiconductors at high concentrations of the donor impurity, near the Mott transition. In this case the wave functions of different donor electrons begin to overlap, and the individual donors can no longer be regarded as independent of one another. Under these conditions one expects that a macroscopic magnetic moment can arise in the magnetic-impurity subsystem. At still higher

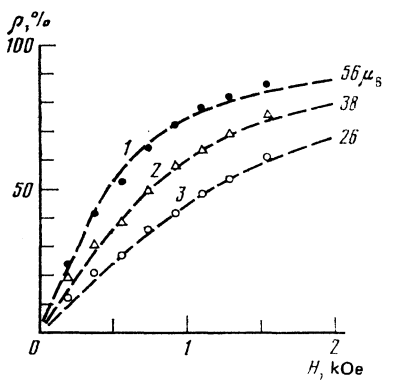

FIG. 7. Degree of circular polarization ρ of the Stokes components of the SFRS as a function of the magnetic field at $T = 1.8$ K. Curves 1, 2, and 3 correspond to the spectral positions indicated by arrows 1, 2, and 3 in Fig. 4. The dashed curves show the functions $W(x)$ approximating the experimental dependence [see formula (14)]. The numbers at the right of the curves indicate the values obtained for the effective magnetic moment of the magneitc-impurity subsystem.

concentrations of the donor impurity the carriers in the semiconductor form a degenerate Fermi system. Such a system would represent a qualitatively new object of study for investigating exchange effects in semimetallic semiconductors.

In closing, we wish to thank M. P. Kulakov for growing the $Cd_{1-x}Mn_xS$ crystals used in this study.

[1]R. R. Galazka, Proc. Fourteenth Intern. Conf. on Physics of Semiconductors, Edinburgh, 1978, publ. by Institute of Physics, London (1979), p. 138
[2]A. V. Komarov, S. M. Ryabchenko, O. V. Terletskii, I. I. Zheru, and R. D. Ivanchuk, Zh. Eksp. Teor. Fiz. **72**, 608 (1977) [Sov. Phys. JETP **45**, 318 (1977)].
[3]J. A. Gaj, P. Buszewski, M. Z. Cieplak, G. Fishman, R. R. Galazka, J. Ginter, M. Nawrocki, R. Planel, R. Ranvaud, and A. Twardowski, Proc. Fourteenth Intern. Conf. on Physics of Semiconductors, Edinburgh, 1978, publ. By Institute of Physics, London (1979), p.1113.
[4]S. I. Gubarev, Zh. Eksp. Teor. Fiz. **80**, 1174 (1981) [Sov. Phys. JETP **53**, 601 (1981)].
[5]A. V. Komarov, S. M. Ryabchenko, Yu. G. Semenov, B. D. Shanina, and N. I. Vitrikhovskii, Zh. Eksp. Teor. Fiz. **79**, 1554 (1980) [Sov. Phys. JETP **52**, 783 (1980)].
[6]D. L. Alov, S. I. Gubarev, V. B. Timofeev, and B. N. Shepel', Pis'ma Zh. Eksp. Teor. Fiz. **34**, 76 (1981) [JETP Lett. **34**, 71 (1981)].
[7]M. Nawrocki, R. Planel, C. Fishman, and R. Galazka, Phys. Rev. Lett. **46**, 735 (1981).
[8]D. G. Thomas and J. Hopfield, Phys. Rev. **175**, 1021 (1968).
[9]Y. Yafet, Phys. Rev. **152**, 858 (1966).
[10]M. A. Krivoglaz, Usp. Fiz. Nauk **111**, 617 (1973) [Sov. Phys. Usp. **16**, 856 (1974)].
[11]E. L. Nagaev, Fizika Magnitnykh Poluprovodnikov [Physics of Magnetic Semiconductors], Nauka, Moscow (1979).
[12]T. Dietl and J. Spalek, Phys. Rev. Lett. **48**, 355 (1982).

Translated by Steve Torstveit